Progress Report #4
July 1, 1983 to February 29, 1984
Cooperative Agreement
NASA No. NCCI-62

Development of Improved Coating for Advanced Carbon-Carbon Components

by

Y. R. Yamaki and J. J. Brown
Department of Materials Engineering
Virginia Polytechnic Institute and State University
Blacksburg, VA 24061
(703) 961-6777

submitted to

NASA
Langley Research Center
Hampton, VA 23665

Date issued

February, 1984

Mr. Phil Ransom
NASA Technical Officer

REACTION SINTERED SILICON NITRIDE AS A COATING FOR CARBON-CARBON COMPOSITES

by

Yoshio Robert Yamaki

(ABSTRACT)

Reaction sintered silicon nitride (RSSN) was studied as a substitute coating material on the carbon-carbon material (RCC) presently used as a heat shield on the space shuttle, and on advanced carbon-carbon (ACC), a later development. On RCC, RSSN showed potential in a 538°C (1000°F) screening test in which silicon carbide coated material exhibits its highest oxidation rate; RSSN afforded less protection to ACC because of a larger thermal expansion mismatch. Organosilicon densification and metallic silicon sealing methods were studied as means of further increasing the oxidation resistance of the coating, and some improvement was noted when these methods were employed.

Acknowledgements

Firstly, the candidate wishes to express his gratitude to his parents, Yoshio and Norma Shimaura Yamaki, for their ever present encouragement and support.

Deepest thanks go to C. W. Spencer, Head of the Department of Materials Engineering, and to committee members J. J. Brown, Chairman, W. R. Hibbard, and J. L. Lytton. Also responsible for widening the candidate's scientific perspectives are D. W. Dwight, G. V. Gibbs, D. P. H. Hassellman, C. T. Herakovich, M. R. Louthan, G. Ulrich, and T. P. Floridis.

This work was funded by a grant from NASA-Langley Research Center, Hampton, Virginia.

Valuable technical assistance was furnished by Steve McCartney and Carlile Price.

Table of Contents

Table of Contents (continued)

List of Tables

List of Figures

List of Figures (continued)

I. Introduction

The space shuttle orbiter is the first application of reuseable heat shield materials. Peak reentry temperatures of approximately 1500°C are encountered by the nose cap and wing leading edges, and carbon fiber-carbon matrix (carbon-carbon) composites are used to provide thermal protection in these areas. The high temperature strength retention and low density of carbon are well suited to aerospace applications, however, protection against oxidation at high temperatures is of paramount importance in a reuseable heat shield system.

High temperature oxidation protection is currently provided by a silicon carbide layer formed on the surface of the carbon-carbon heat shields by a reactive penetration into the shield itself. In the coating process, the entire component is covered by a mixture of silicon, silicon carbide, and alumina powders and heated to approximately 1700°C for several hours. During cooling, however, tensile stresses build in the coating due to a thermal expansion mismatch with the unreacted substrate beneath, and cracking of the coating occurs. Such coating defects limit heat shield life by permitting oxidation of the underlying material.

The primary source of the thermal expansion mismatch is the orientation of graphite fibers in the composite. The shield consists of layers of graphite fiber cloth which are oriented parallel to the outer surface and are bonded together and impregnated by the amorphous carbon matrix.

The carbon-carbon composites for the shuttle program are manufactured by the Vought Corporation, and two types of composites have been produced. A material designated reinforced carbon-carbon (RCC) is currently used on the shuttle orbiters; however, a second type, designated advanced carbon-carbon (ACC) is under study for future use because of its improved oxidation and mechanical properties. RCC and ACC differ in the type of graphite fiber used, the weave pattern of the cloth, and in the agents used to densify their matrices.

Dilatometer measurements on RCC have indicated that the coefficient of thermal expansion is $4.7 \times 10^{-6}/^{o}C$ (25 - 800°C) perpendicular to the plies but only $1.4 \times 10^{-6}/^{o}C$ (25 - 800°C) in the direction parallel to the plies and the shield surface. A figure of $4.7 \times 10^{-6}/^{o}C$ (25 - 800°C) is obtained for material which has been converted to SiC and varies little with respect to orientation.

Oxidation due to coating cracks is currently being retarded by the application of a crack sealing overcoat. While this does result in a large improvement in oxidation resistance, the most desireable approach would be to eliminate or at least reduce the residual coating stresses such that cracks are not formed.

The objective of this effort is to improve the oxidation resistance of carbon-carbon composites through the use of an alternative coating material-reaction sintered silicon nitride (RSSN). This material reportedly possesses a lower coefficient of thermal expansion than silicon carbide, and it can be processed at lower temperatures. Both of these factors should contribute to a reduction of residual coating stresses. However, as-processed RSSN is porous, and means

to alleviate problems associated with this porosity were also investigated.

II. Review of Literature

This highly desireable properties of a material for coating carbon-carbon composites would include a thermal expansion coefficient slightly lower ($\leq$ 10%) that of the composite, low density, and chemical and physical stability in oxidizing and low pressure environments from room temperature to well above 1600°C. A review of the literature reveals that there is practically no material which can provide such a combination of properties.

For the purposes of selecting a material for study as a coating for carbon-carbon, the following properties were considered: 1) improved thermal expansion match with the substrate; 2) thermal stability and oxidation resistance; 3) ability to coat the substrate. The materials reviewed were Si_3N_4, Si_2ON_2, and sialons. Among these, Si_3N_4 was selected as the best candidate for research.

A. Silicon Nitride

Silicon nitride bodies can be formed by three methods: reaction sintering (RS), chemical vapor deposition (CVD), and hot pressing (HP). There are two modifications of the nitride, designated alpha and beta. The alpha phase is obtained when nitrogen reacts with silicon below its melting point (1410°C). The beta phase is formed when the nitride is precipitated from molten silicon containing dissolved nitrogen (1). Although reported values of coefficient of thermal expansion for silicon nitride vary widely, all are below that measured for the present SiC coating. Some values are listed in Table 1.

TABLE 1

Comparison of Si_3N_4 Thermal Expansion Data

α	form	range	reference
$2.4 \times 10^{-6}/^{\circ}C$	RS, 70% dense	21-982°C	2
$2.75 \times 10^{-6}/^{\circ}C$	HP, 73.0 g/cc 70-100% β	21-982°C	2
$2.47 \times 10^{-6}/^{\circ}C$	not given	25-1000°C	3
$3.1 \times 10^{-6}/^{\circ}C$	RS		4
$3.5 \times 10^{-6}/^{\circ}C$	β	0-1000°C	4
$3.61 \times 10^{-6}/^{\circ}C$, a-axis	α	0-1000°C	5
$3.70 \times 10^{-6}/^{\circ}C$, c-axis			
$3.23 \times 10^{-6}/^{\circ}C$, a-axis	β	0-1000°C	5
$3.72 \times 10^{-6}/^{\circ}C$, c-axis			

Reaction sintered silicon nitride (RSSN) is produced by heating compacted silicon powder in nitrogen. The advantages of the RS process include simplicity and little dimensional change (< 0.1%) on nitridation (4). Reaction sintering can be accomplished by two basic types of processing: the single stage or two stage process (7). In the single stage process, silicon is reacted completely with nitrogen below the melting point of silicon; the two stage process comprises partial nitridation below the melting point of silicon followed by completion of nitridation above the melting point. The two stage process shortens nitridation time in large bodies; however, this should not be a critical factor in the formation of a thin layer of RSSN. The product of the single stage process is primarily alpha silicon nitride whereas the two stage process produces a mixture of alpha and beta. Although the beta phase reportedly possesses higher oxidation resistance (6) and a lower coefficient of thermal expansion, the strength of RSSN reportedly increases with increasing alpha content (4,7). The higher process temperatures required to produce the beta phase would probably also result in higher residual coating stresses on cooling.

The oxidation rate of RSSN is higher than that of either HP or CVD silicon nitride until a continuous silica layer is formed within the pores (4,8). After this layer forms, RSSN exhibits a lower rate of oxidation than HP material, and it can almost match that of CVD material due to its high purity. It is possible to reduce or eliminate the porosity of RSSN by two methods.

One method involves melting and impregnating the surface of RSSN with liquid silicon. This has been shown to markedly increase the oxidation resistance of RSSN (9), and the presence of free silicon reportedly inhibits the high temperature decomposition of silicon nitride (10). The ability of liquid silicon to wet silicon nitride can be enhanced by alloying elements (11) as well as high temperatures and low pressures (12). A second method of increasing the density of the product involves impregnation with a silicon and nitrogen containing organo-metallic, followed by high temperature decomposition to leave silicon nitride within the impregnated porosity (13).

Another method of producing silicon nitride is by CVD techniques. The CVD material is usually produced by heating a flowing mixture of a silicon halide, often $SiCl_4$, and ammonia in a reaction vessel. A range of microstructures can be obtained by varying deposition conditions and either amorphous or alpha silicon nitride can be formed.

A potential problem in the use of silicon nitride in contact with carbon at high temperatures is reaction between the two materials to form silicon carbide. Billy and Colombeau (4) have reported that alpha silicon nitride and carbon react above 1400°C; however, in studies of CVD silicon nitride deposited on graphite substrates, Galasso (14) reported a reaction between the two materials above 1600°C. Gebhardt et al. (15) carried out mass spectrometer studies of the thermal stability of amorphous and crystalline CVD silicon nitride and found that decomposition begins at 1450-1500°C.

Though CVD silicon nitride possesses favorable properties, it was not pursued as a coating method because of the relatively complex

apparatus required, and because it would later have to be scaled up to coat the actual heat shield parts, some of which are quite large and complex. This would probably present an entirely new set of problems in actual practice.

Uniaxial hot pressing of silicon nitride powders with sintering aids such as MgO or Y_2O_3 is probably the most common method of producing silicon nitride bodies in industry. However, uniaxial hot pressing would be unsuitable for coating large complex parts of limited strength. Isostatic hot pressing may be viable as a coating method but would be extremely expensive and would be beyond the reach of available resources.

B. Silicon Oxynitride

Silicon oxynitride (Si_2ON_2) is similar in properties to silicon nitride and is sometimes present as an oxidation product of the nitride; its presence is apparently dependent on the form of the nitride and on the oxidizing conditions (4,5,16). X-ray studies by Henderson (5) indicate that the coefficient of thermal expansion of the oxynitride is quite close to that of the nitride with the exception of the oxynitride α-axis; in this direction the value is approximately one-third of that measured in other directions. Washburn (16) reports that the oxynitride has higher oxidation resistance than the nitride; however, this is based on the use of impure samples containing both the nitride and oxynitride as well as the carbide.

RS silicon oxynitride can be produced by nitridation of silicon-silica mixtures (5,17) although not by direct reaction of silica and silicon nitride (16). Amorphous Si-O-N deposits have been prepared

by vapor deposition (18) with mixtures of NO, NH_3, and SiH_4, and the composition range from SiO_2 to Si_3N_4 is accessible. These compositions were studied in the context of electronic devices, however.

One area in which the oxynitride seems definitely inferior to the nitride is that of high temperature stability under vacuum. Ehlert et al. (17) found that decomposition became detectable at less than 1000°C by mass spectrometry using specimens produced by the nitridation of a 3:1 Si-SiO_2 mixture. The decomposition products were silicon monoxide, nitrogen, and significantly, silicon nitride. This decomposition to the nitride makes the oxynitride definitely less attractive for high temperature, low pressure applications such as heat shields.

C. Sialons

The sialons are a class of materials most often produced by reacting mixtures of silicon nitride, alumina, and often aluminum nitride. The literature in this material is predominantly concerned with material formed by hot pressing, a method which has been rejected as a coating technique for the purposes of this research. Additionally, due to the presence of sintering aids, oxidation rates in HP sialons are subject to a major increase over those of high purity materials (4,19). HP sialons show about the same oxidation resistance as RSSN.

Pressureless sintered sialons have been prepared when the compacts were covered with a buffer mixture of silicon nitride and alumina or silica (20); however, the temperature utilized (1800°C) was beyond the reach of available resources if any precise process

control was to be exercised. No information on the oxidation resistance of pressureless sintered sialons or on the application of such materials as coatings was found.

III. Materials and Methods

A. Carbon-Carbon Substrates

1. Reinforced Carbon-Carbon (RCC)

RCC (Vought Corporation) comprises plies of rayon-derived, square weave graphite cloth in a cross ply configuration and a matrix derived from both phenolic resin and furfuryl alcohol. In the manufacturing process, phenolic impregnated graphite cloth plies are bonded, cured, and then pyrolyzed to form a low density, low strength carbon-carbon material. Repeated impregnation and pyrolyzation cycles utilizing furfuryl alcohol increase strength and density. Final impregnation with tetraethyl orthosilicate (TEOS) is followed by heating to yield amorphous silica within any porosity. This serves to increase oxidation resistance.

The RCC specimens used in this research were cut from pieces which had been coated with silicon carbide and treated with TEOS. The coating was sliced away to provide a fresh surface for coating experiments. As mentioned earlier, the coefficient of thermal expansion of such material was determined to be $1.4 \times 10^{-6}/^{\circ}C$ from 25 - $800^{\circ}C$ in the critical direction. A Dupont Model 943 Thermomechanical Analyzer was utilized. Measurements done by Vought Corporation (method not indicated) indicate a figure of $2.3 \times 10^{-6}/^{\circ}C$ over approximately the same temperature range.

2. Advanced Carbon-Carbon (ACC)

ACC is being considered as a replacement for RCC because of its better mechanical and oxidation properties. The starting material is phenolic impregnated, eight harness weave Fiberite graphite fiber

cloth derived from polyacrylonitrile. The manufacturing process for ACC is basically the same as that for RCC except that phenolic resin is used as a densifying agent rather than furfuryl alcohol.

In contrast to the available RCC material, the ACC material was neither TEOS impregnated nor silicon carbide coated. It was in the form of a 0.1" thick sheet.

Measurements by Vought Corporation indicate a critical coefficient of thermal expansion of only $1.1 \times 10^{-6}/^{o}C$ from 27 to $815^{o}C$.

B. Coating Furnace

The coating furnace consisted of a high purity alumina furnace tube used in conjunction with silicon carbide heating elements. The tube was closed at one end, while at the opposite end, high temperature silicone adhesive was used to attach high vacuum glass hardware. The apparatus is shown in Figures 1 and 2. Not shown in Figure 2 are water cooling coils used to protect the silicone adhesive from excessive temperatures.

Process atmospheres were established by several cycles of evacuation to 150 - 300 microns pressure, followed by backfilling with "Drierite" treated gas. As furnace heat-up proceeded, the tube was subjected to a purge during which 4 -5 cubic feet of gas flowed through the tube over a period of 1 - $1\frac{1}{2}$ hours. At the end of the purge, gas flow was reduced to 50 - 70 cc/min for the duration of processing. Both static and flowing atmospheres were available to suit the ongoing processing, and an optical curve follower type controller was used to provide desired heating and cooling rates. A $3^{o}C$/min. heating rate was used unless otherwise stated.

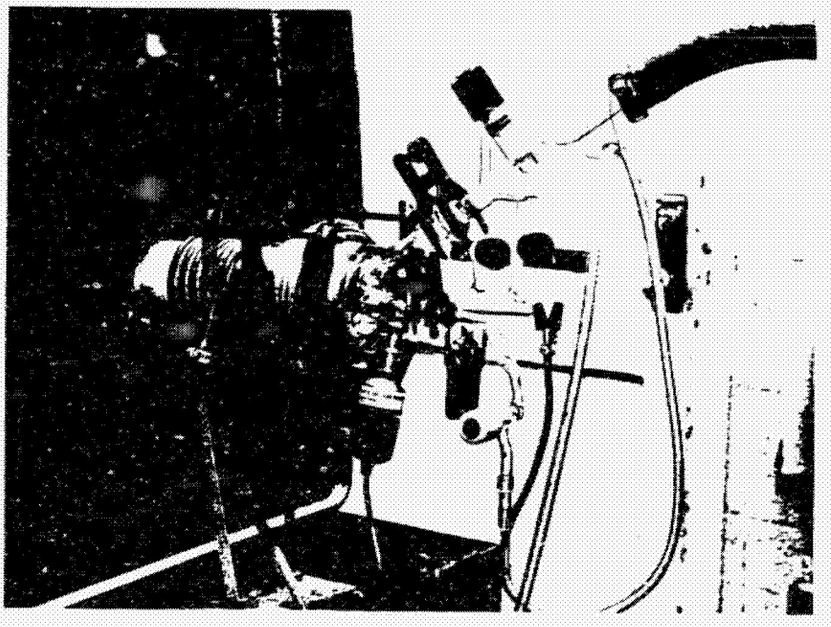

Figure 1. Coating apparatus and furnace.

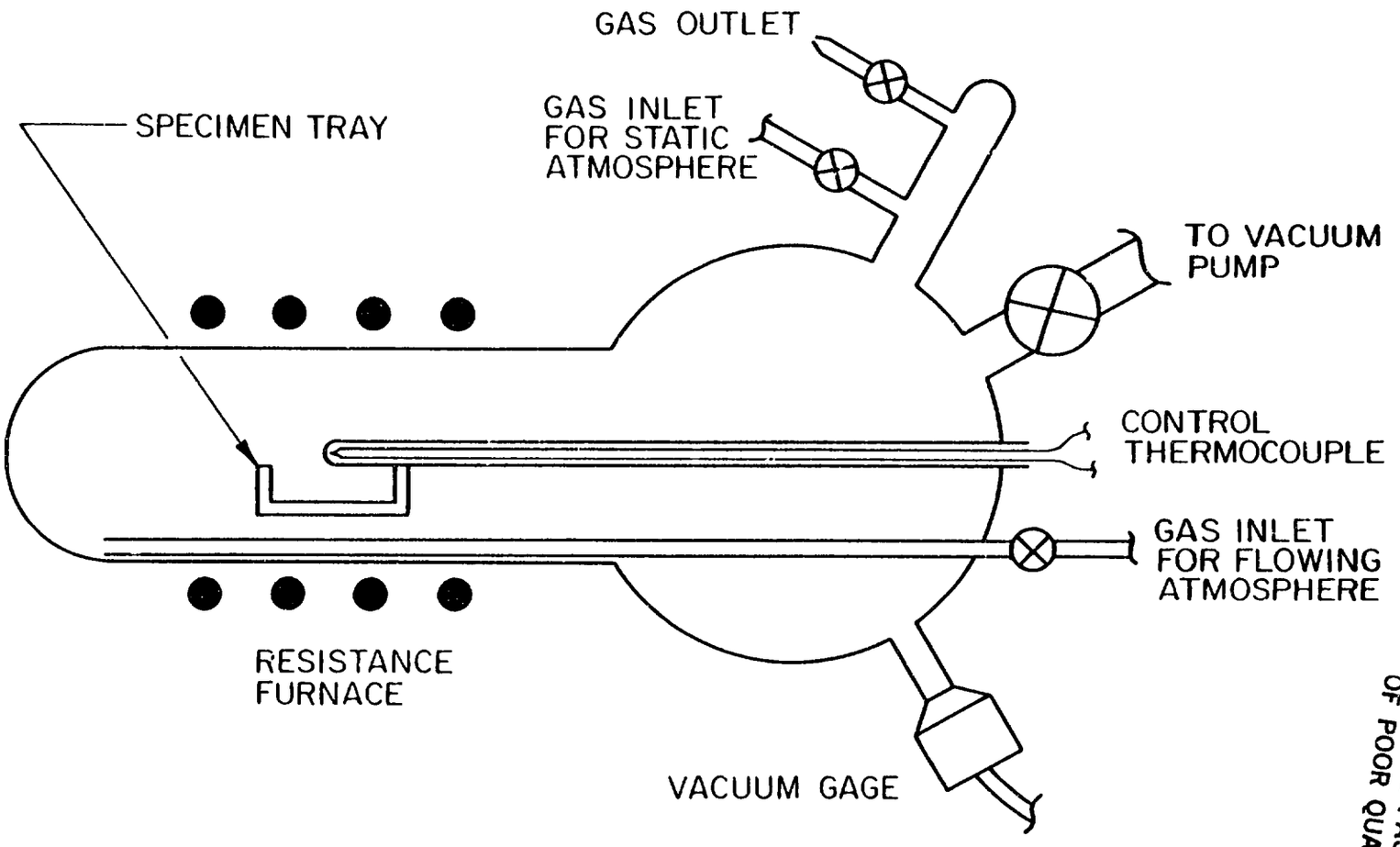

FIGURE 2. SCHEMATIC OF COATING APPARATUS.

C. Oxidation Test Procedure

The oxidation test procedure was based on general guidelines obtained during ground-based oxidation mass loss measurements conducted by the Vought Corporation. The currently used heat shield material exhibits its highest mass loss rate in a 1000°F test conducted in air, with weighings every six hours.

For this research, oxidation test specimens were supported on a parallel gridwork of $\frac{3}{16}$" diameter mullite rods spaced $\frac{3}{8}$" between centers and fixed $\frac{1}{2}$" above the surface of an insulating refractory carrier block. Tests were carried out in air in a 1000°F muffle furnace, with weighings every six hours. The refractory block was preheated before any specimens were introduced into the furnace.

IV. Materials and Methods: RCC

The coatings for RCC were of three types: a basic RSSN coating, an organosilicon densified RSSN coating, and a silicon sealed RSSN coating. Both the densified and sealed coatings were produced by additional treatments to the basic coating.

A. Basic Coating

The basic RSSN coating for RCC was produced in the following manner:

1) The existing silicon carbide coating was sliced away from the furnished material and specimens were cut to a 0.70" x 0.22" x 0.12" nominal size. The plies were parallel to the 0.70" x 0.22" face.
2) The surface of the specimens was roughened by heating to 600°C for 10 minutes in air. A roughening effect occurs because the matrix carbon oxidizes at a much higher rate than the fibers.
3) Any loose material left on the surface was removed, and the specimens were treated with dilute HF to remove from the surface any silica resulting from the TEOS treatment.
4) Each specimen received a light dip coating in a 5 micron average particle size silicon-acetone slurry.
5) Specimens were placed into the furnace and heated to 1450°C for 45 min. in one atmosphere of flowing argon.
6) Any residue was removed by ultrasonic cleaning in aceton and gentle wiping, as necessary.

7) Each specimen received repeated dip coating in silicon-acetone slurry until a coating thickness of 0.04 inch was reached.

8) The specimens were heated to 1350°C for 12 hours in one atmosphere of static nitrogen.

B. Densified Coating

The organosilicon material used to densify the coatings was hexaphenyl-tricyclosilazane. It was prepared from diphenyldichlorosilane and ammonia as described by Mazdiyasni et al. (10), who used the term "silazane" in referring to it.

The silazane used for the densification of the coatings was prepared in a flask topped by a refluxing condenser. A solution of diphenyldichlorosilane in toluene (approx. 1:5) was heated to 110° - 120°C in the flask by partial immersion in a stirred ethylene glycol bath. Ammonia gas was bubbled through the hot solution by means of a glass tube inserted down the bore of the condenser, and a precipitate, assumed to be ammonium chloride, formed in the solution as soon as the ammonia was introduced. After the reaction was allowed to proceed for approximately five hours, the contents of the flask were filtered, and the chloride precipitate was discarded. The filtrate was then chilled to precipitate the silazane, and the toluene and silazane were stored together in a refrigerator. Before use, excess toluene was pressed from the silazane crystals between two layers of filter paper, and the crystals were allowed to air dry.

Vacuum impregnation of the samples took place in a glass tube which could be heated in a small vertical oven. Samples were placed

in the tube with dry silazane, and the tube was then lightly evacuated and backfilled with nitrogen several times. The samples were slowly heated, and when the silazane had melted completely, the tube was evacuated and backfilled an additional time to ensure complete impregnation. Heating was continued until a temperature of approximately 275°C was reached, and maintained for five hours. The samples were then moved to the coating furnace where they were heated in flowing nitrogen at a rate of 2°C/min. to 600° and 3°C/min. to 1400°C, where they were held for one hour then slowly cooled.

C. Sealed Coating for RCC

The coatings of some of the specimens were subjected to a silicon sealing treatment to improve oxidation resistance. After the basic RSSN coating was complete, the specimens were given a light dip coating in an acetone slurry of -325 mesh boron powder. This was followed by dip coating in the silicon slurry and heating to 1450°C for two hours under flowing argon.

D. RCC Specimen Designations

Specimens are grouped according to the type of coating employed. Capital letters indicate group and dashed numerals indicate individual specimens. The designations for RCC specimens are as follows:

Type A: 0.04" RSSN coating/oxidized substrate.

B: Silazane densified A type coating.

C: Boron-silicon sealed A type coating.

V. Results: RCC

A. Results of RCC Coating Tests

To improve coating adhesion, the uncoated RCC specimens were roughened by oxidation at 600°C for 10 minutes. Prior tests and SEM examinations of small specimens oxidized in a silica boat indicated that these conditions would be suitable; however, the actual test specimens were suspended by platinum wire to expose the entire surface area. The difference in heating conditions gave different results; the actual test specimens were over-oxidized and the degree of oxidation varied depending on placement within the furnace. Initially, the mean specimen weight was 0.511 grams with a standard deviation of 0.006 grams; after the oxidation treatment the mean and standard deviation were 0.437 grams and 0.015 grams, respectively. The oxidized surfaces were noticeably fragile in most cases, and any loose material was removed before the post oxidation weighing. Since the supply of substrate material was limited, only the most severely oxidized RCC specimens were discarded, and the remainder utilized for the purpose of comparing coating treatments.

1. Basic Coating

The basic RSSN coating was successfully applied to the RCC substrates with no apparent cracking. Figures 3 and 4 show the typical fibrous appearance of the RSSN free surface. A well bonded interface between the coating and substrate can be seen in Figure 5. Figure 6 is included for comparison with a coating applied to a non-oxidized RCC surface. The relatively smooth cavities in the interior of the coating are caused by air entrapment during the dip coating of

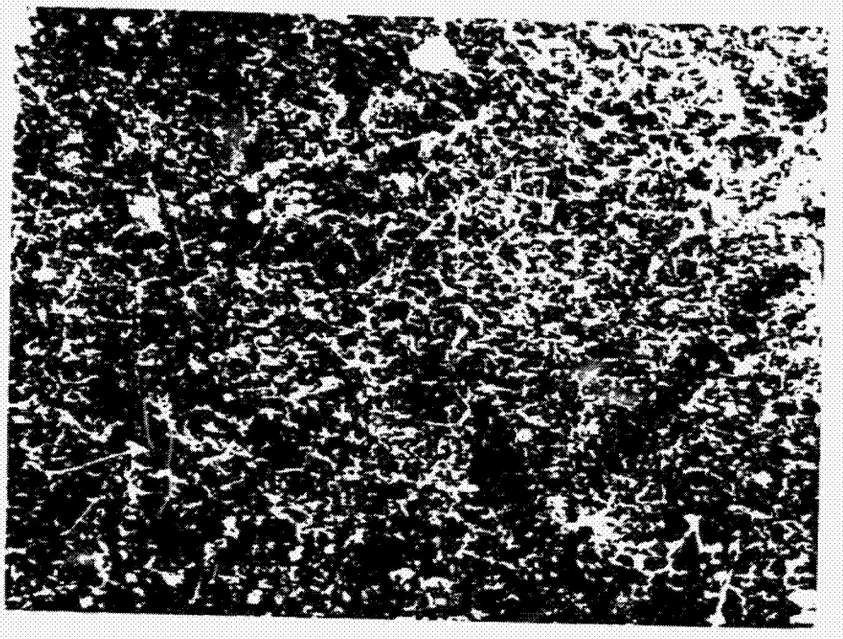

Figure 3. Type A coating surface, 200 X.

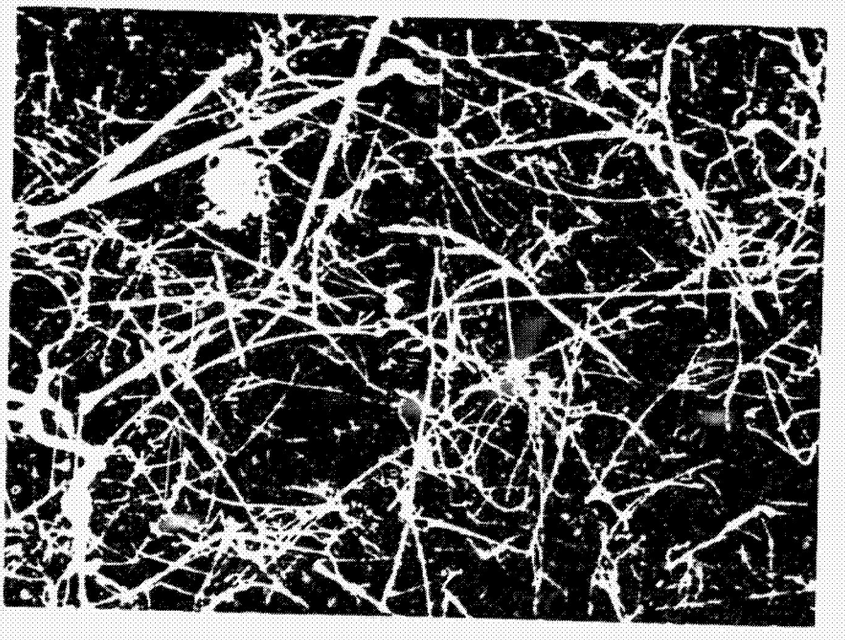

Figure 4. Type A coating surface, 2000 X.

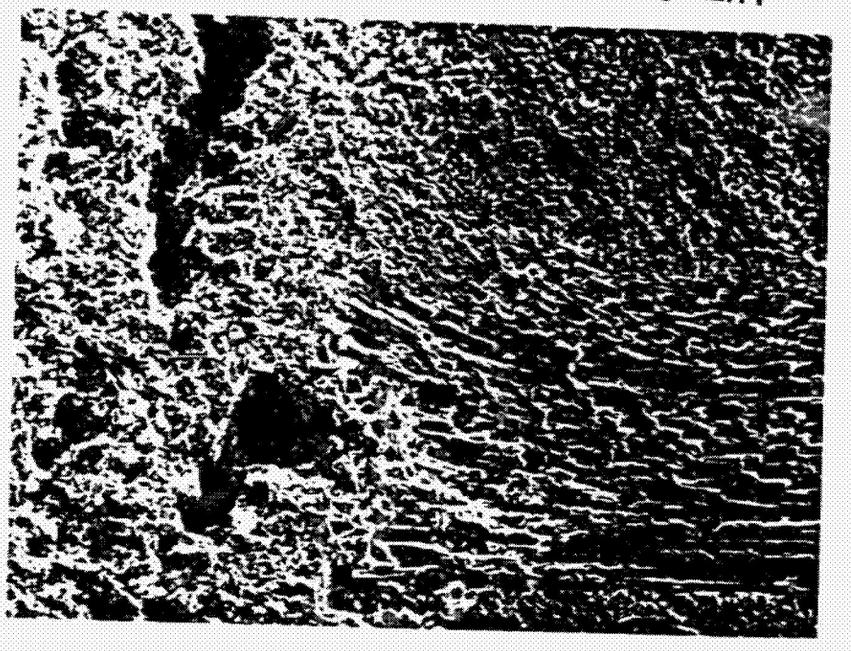

Figure 5. Type A coating-substrate interface, 200 X.

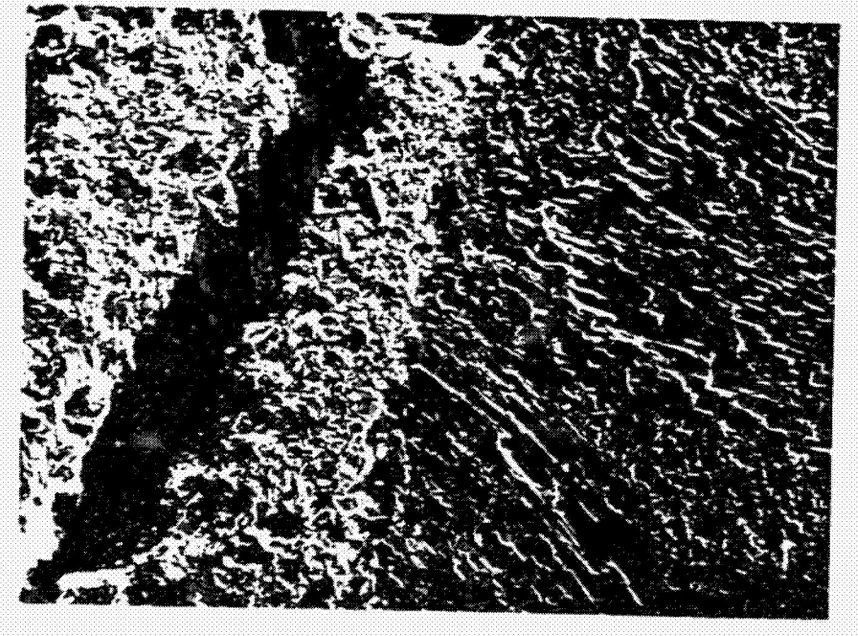

Figure 6. Coating-substrate interface, unprepared substrate, 200 X.

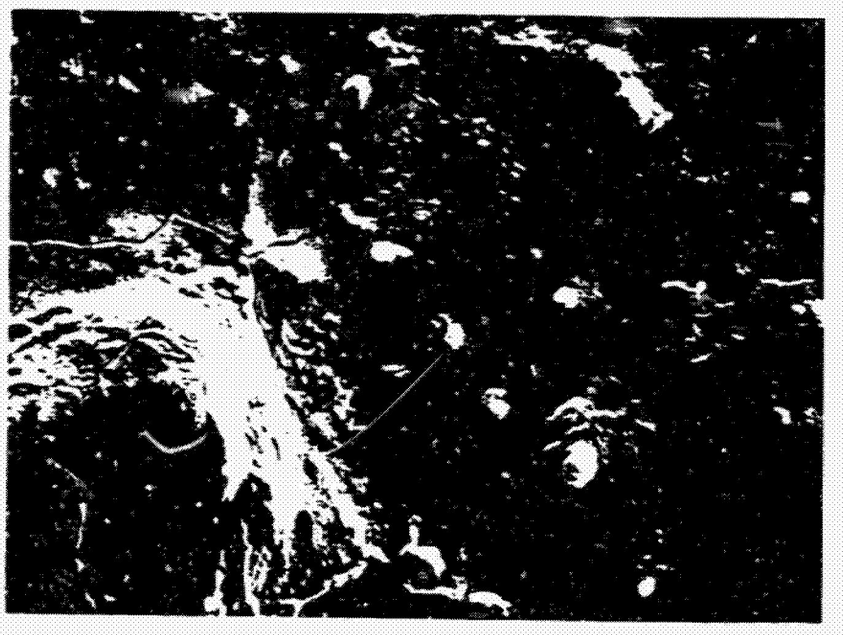

Figure 7. Type B coating surface, 2000 X.

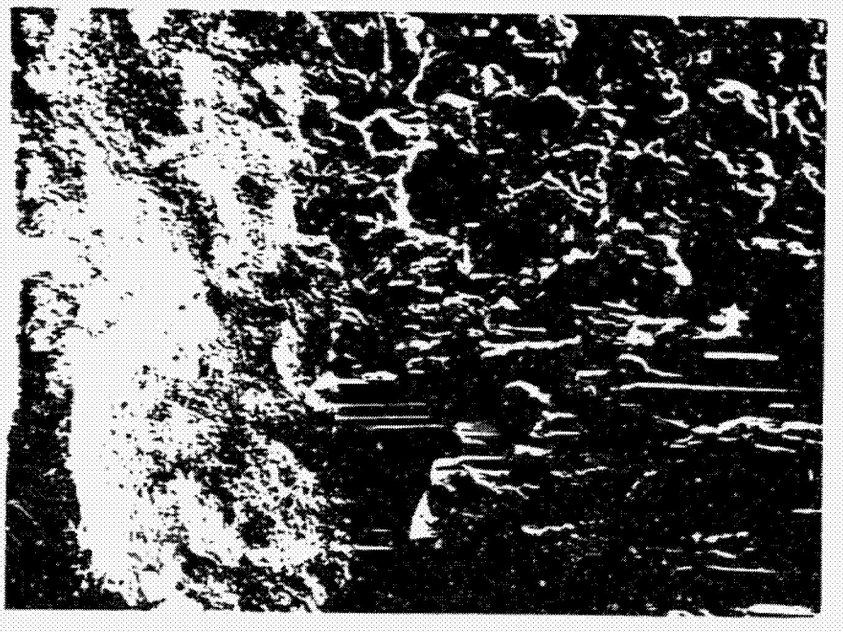

Figure 8. Type B coating-substrate interface, 2000 X.

the specimen.

2. Densified Coating

The results of the coating densification treatment for RCC were highly variable even though the specimens for specific coating/oxidation screening tests were processed together. The microstructure of the densified coatings was in many cases apparently unchanged from that of the basic RSSN coating; however, in other cases the change in structure was quite obvious. Figures 7 and 8 show portions of a specimen exhibiting a large degree of structural change due to the coating densification treatment. This speciman was not used in oxidation tests.

3. Sealed Coating for RCC

The boron-silicon surface sealing procedure was partially successful for RCC samples; however, only two samples were available and their edges were fused together during the sealing procedure. An initial treatment produced approximately 80% surface coverage, and an additional treatment increased coverage to over 95%. The specimens were subjected to a low temperature oxidation test in this fused, partially scaled condition.

B. Results of RCC Oxidation Tests

There is some difficulty in comparing the results for the various types of specimens to existing data because of their small size and varying shapes. Mass loss figures for standard SiC coated ACC are given in units of lb/ft^2. This type of calculated data is readily obtained for large specimens; however, an accurate figure of this type is difficult to obtain for small specimens with rounded edges. Mass

losses are therefore compared among specimens on an average percentage basis in Figure 9. Individual mass and mass losses for those specimens which were tested are given in Table 2.

Average mass loss/area figures are listed in Table 3 for rough comparison with the typical loss figure of 0.013 lb/ft^2 in six hours at 1000^oF in air obtained for ACC which has been TEOS impregnated, SiC coated, and sealed by Vought Corporation. These figures are based on nominal surface areas and should therefore be considered approximations.

1. Basic Coating

Figure 10 shows the effect of both the substrate priming procedure (basic coating steps 4 and 5) and the oxidation tests on RCC substrate. The dense layer of substrate fibers is probably a result of increased oxidation resistance of a thin surface layer of Si and SiC formed by the priming procedure. The loose fibers are the result of preferential oxidation of the substrate matrix. The relatively smooth cavity is due to air trapped during dip coating.

2. Densified Coating

As mentioned earlier, results for the silazane densified coatings have been inconsistent. Figure 11 shows an apparently high coating density adjacent to the substrate in specimen B-4, which exhibited the lowest mass loss of any specimen. Figure 12 shows specimen B-1, which was also densified but did not exhibit appreciably improved oxidation resistance. The surface of the coatings of B-1 and B-4 were quite similar and a typical appearance is shown in Figure 13. Note that this surface is much rougher than that shown in Figure 7.

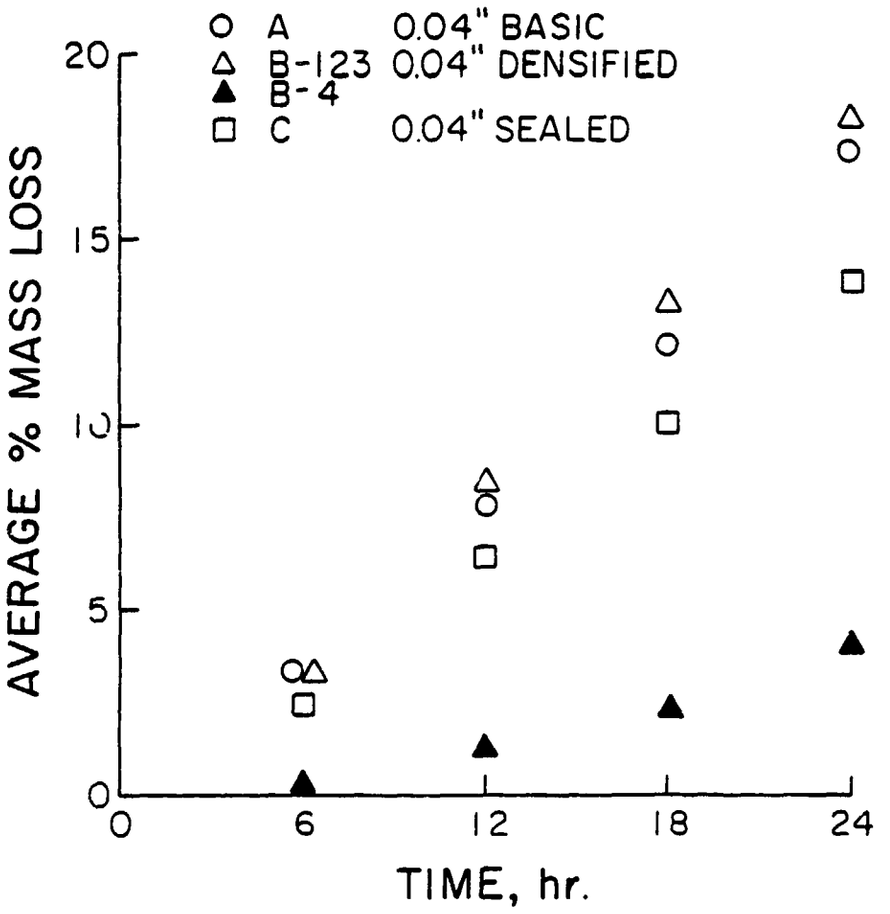

FIGURE 9. 1000 F MASS LOSS FOR TYPES A,B,C.

TABLE 2

Coated Mass and Mass Loss for Individual RCC Specimens

Specimen	Coated Mass, g	Total Mass Loss, g(%), at Time, hr. 6	12	18	24
A - 1	0.8176	0.0349 (4.26)	0.0720 (8.81)	0.1092 (13.36)	0.1542 (18.86)
2	0.7831	0.0209 (2.67)	0.0511 (6.53)	0.0826 (10.55)	0.1198 (15.30)
3	0.8115	0.0259 (3.19)	0.0638 (7.86)	0.1004 (12.37)	0.1441 (17.76)
avg.		(3.35)	(7.73	(12.09)	(17.31)
B - 1	0.8633	0.0248 (3.29)	0.0692 (8.02)	0.1088 (12.60)	0.1513 (17.53)
2	0.8385	0.0262 (3.12)	0.0668 (7.97)	0.1071 (12.77)	0.1492 (17.79)
3	0.8545	0.0293 (3.43)	0.0766 (8.96)	0.1211 (14.17)	0.1648 (19.29)
avg.		(3.28)	(8.32)	(13.18)	(18.20)
B - 4	0.9862	0.0039 (0.40)	0.0118 (1.20)	0.0230 (2.33)	0.0395 (4.01)
C	1.9211	0.0470 (2.44)	0.1233 (6.42)	0.1920 (9.99)	0.2661 (13.85

TABLE 3

Calculated RCC Mass Loss/Area for 6 hr. Oxidation at 1000°F in Air

Specimen	Nom. Area, in^2	6 hr. Avg. Loss, g	6 hr. Mass Loss, lb/ft^2
A123 Avg.	0.76	0.0272	0.011
B123 Avg.	0.76	0.0268	0.011
B4	0.76	0.0039	0.0016
C	1.37	0.0470	0.011

Figure 10. Type A coating-substrate interface, oxidized 24 hours at 1000°F, 200 X.

Figure 11. Specimen B-4 coating-substrate interface, oxidized 24 hours at 1000°F, 200 X.

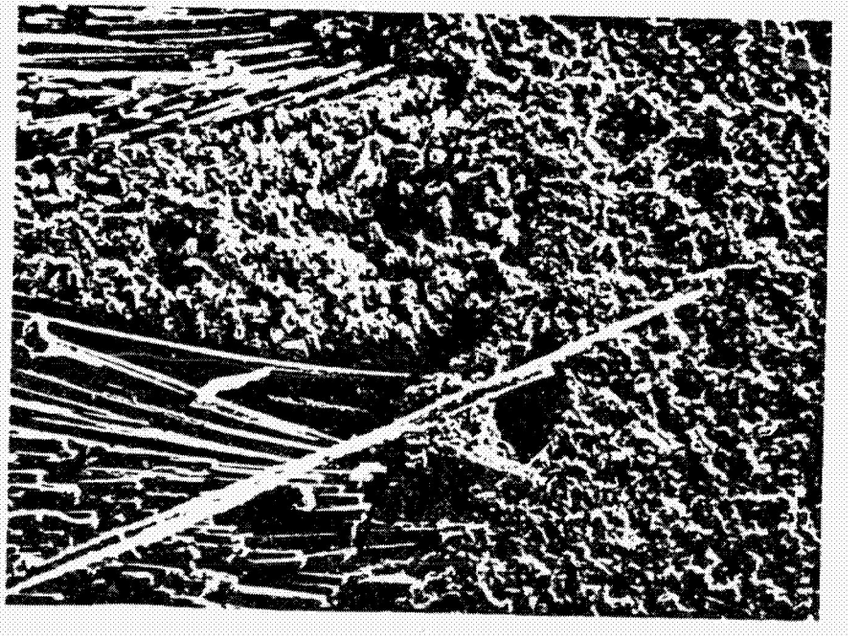

Figure 12. Specimen B-1 coating-substrate interface, oxidized 24 hours at 1000°F, 200 X.

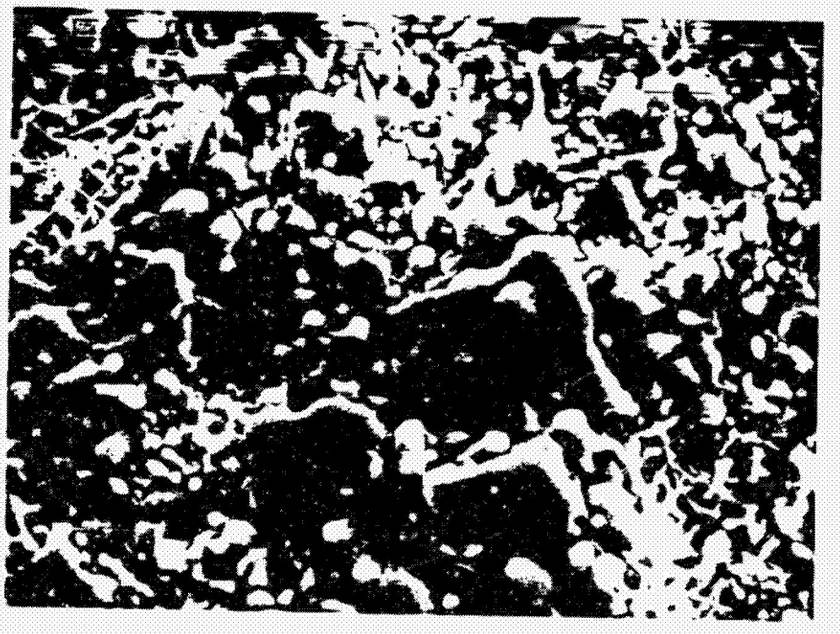

Figure 13. Type B coating surface, oxidized 24 hours at 1000°F, 200 X.

The difference is most probably due to processing differences rather than to oxidation (the surface shown in Figure 5 is unoxidized).

3. Coating Sealant

Despite incomplete surface coverage, the boron-silicon surface sealant did result in improved oxidation resistance on a weight percentage basis but not on the approximate mass loss/area basis. Figure 14 indicates good potential for this method, however, and shows the interior and some of the outer surface of a sealed sample which has been sectioned. The faceted fracture band represents sectioned sealant on the surface while the relatively smooth area below it is impregnated coating material. Figure 15 is a higher magnification view of the sealed layer. Figure 16 shows the outer surface of a sealed specimen while Figure 17 shows the typical appearance of the coating-substrate interface for an oxidized specimen.

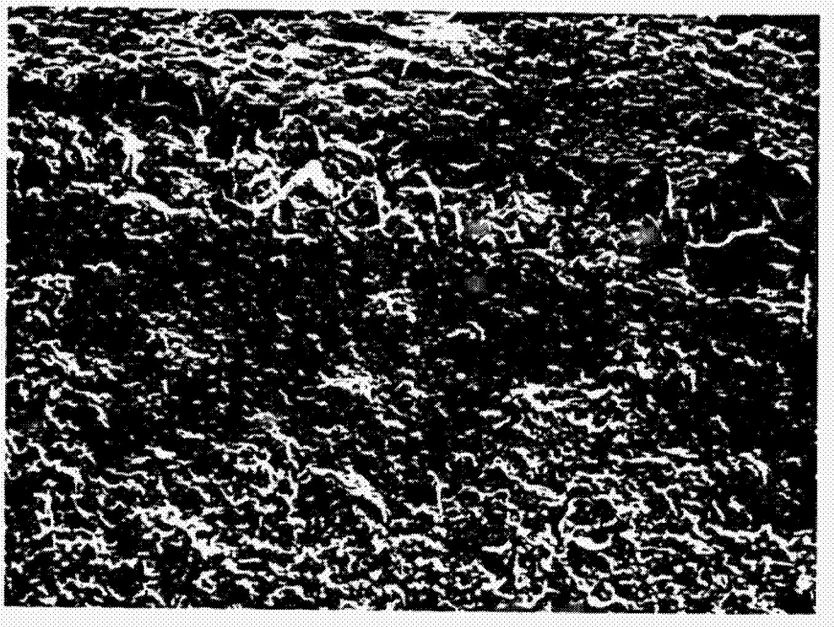

Figure 14. Type C coating section, sealed layer, oxidized 24 hours at 1000°F, 200 X.

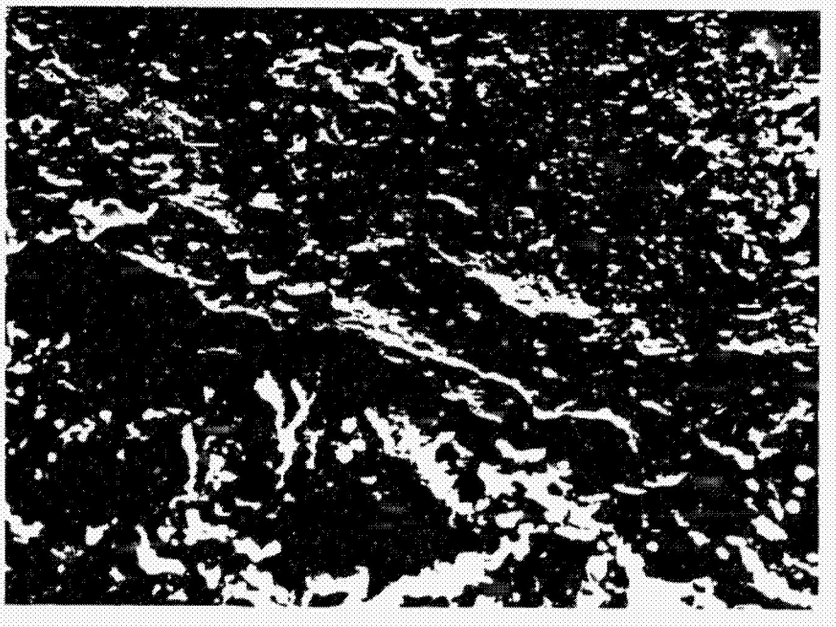

Figure 15. Type C coating section, sealed layer, oxidized 24 hours at 1000°F, 1000 X.

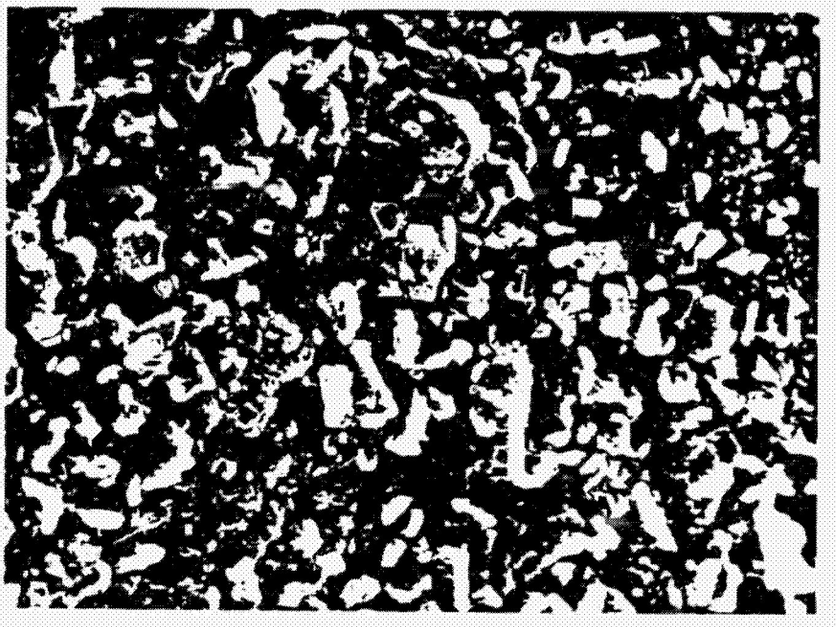

Figure 16. Type C coating surface, 1000 X.

Figure 17. Type C coating-substrate interface, oxidized 24 hours at 1000°F, 200 X.

VI. Materials and Methods: ACC

The procedures used for coating ACC specimens were primarily variations of those used for coating RCC. The different coatings are classified as previously described (basic, densified, and sealed coatings) and are explained below.

A. Basic Coating

A variety of methods were employed to form basic coatings on ACC. Differences occurred in substrate surface preparation, "primer" composition, green coating composition/thickness, and in nitridation time/temperature.

Substrate surface preparation consisted of either abrasive roughening alone or abrasive roughening followed by oxidation roughening. Abrasive roughening was done with 240 grit SiC paper. Material was removed until there were no surface contours visible from the underlying graphite cloth plies, and the edges were rounded. Oxidative roughening consisted of heating specimens to 540°C in air for 20 minutes using the oxidation test conditions.

The "primer" consisted of either 100% 1-5 micron size silicon powder or the silicon powder with 5.0 w/o -325 mesh boron powder.

The boron-containing primer was used with green silicon coatings containing 0, 2.5, or 5.0 w/o boron. Two coating thicknesses, approximately 0.04 inch and 0.02 inch, were utilized for some specimens.

The nitridation temperature/time was also varied in an attempt to lower thermal stresses. Heat treatment ranged from 12 hr./1350°C to 36 hr./1150°C.

B. Densified Coating

Coating densification procedures were identical to those which were used for RCC. However, for ACC, the procedure was repeated three times prior to any oxidation tests.

C. Sealed Coatings

Three coating sealing procedures were employed. All start with a light dip coating in a -325 mesh boron-acetone slurry. Following this, the specimens were either: 1) dipped in the 1-5 micron silicon-acetone slurry and heated to 1450°C for two hours under flowing argon at one atmosphere, 2) dipped in silicon slurry and heated to 1450°C for 45 minutes under argon at 200 to 300 microns pressure, or 3) heated to 1450°C in the low pressure argon atmosphere in contact with -20 mesh silicon granules.

D. ACC Specimen Designations

The ACC specimen designations differ slightly from those of RCC specimens due to the larger variety of specimens. General specimen groups are still designated by a capital letter, any subgroups are designated by a numeral, and individual specimens by a final dashed numeral. Groups D, E, and F are considered basic coatings. Group G contains densified coatings and Group H sealed coatings. The coating types are summarized in Table 4.

The uncoated size of Group D1 specimens was 0.5" x 0.4" x 0.1"; the remainder of the ACC specimens measured 1.0" x 0.5" x 0.1".

TABLE 4

Coating Types for ACC

	Surface Prep.	Primer	Green Coating	Nitridation Temp./Time
D1	240 grit	Si	0.04" Si	1350°C/12 hr.
2	240 grit	Si	0.02" Si	1350°C/12 hr.
3	240 grit + oxidation	Si	0.02" Si	1350°C/12 hr.
E1	240 grit	Si	0.04" Si	1300°C/12 hr.
2	240 grit	Si	0.04" Si	1250°C/18 hr.
3	240 grit	Si	0.04" Si	1200°C/24 hr.
4	240 grit	Si	0.04" Si	1150°C/36 hr.
F1	240 grit	Si + 5.0 B	0.04" Si	1350°C/12 hr.
2	240 grit	Si + 5.0 B	0.04" Si + 2.5 B	1350°C/12 hr.
3	240 grit	Si + 5.0 B	0.04" Si + 5.0 B	1350°C/12 hr.

G Triple silazane densification of D2 type coating.

H1 Boron-silicon surface sealing of D1 type coating;
1-5 micron size Si sealant, 1 atm. argon.

H2 Boron-silicon surface sealing of D2 type coating;
1-5 micron size Si sealant, 200-300 microns pressure.

H3 Boron-silicon surface sealing of D2 type coating;
-20 mesh Si sealant, 200-300 microns pressure.

VII. Results: ACC

A. Results of ACC Coating Tests

1. Basic Coatings

Because all of the coatings which were considered for further study began with the same processing (1350°C nitridation for 12 hours), the coating crack characteristics of all specimens were similar. Three fracture locations were observed.

Observable on the surface of the coating were cracks which run from the coating surface to the coating-substrate interface. These cracks form a specimen-wide network with spacings generally on the order of $\frac{1}{4}$ to $\frac{3}{8}$ inch. There was no strong crack orientation except where cracks sometimes ran parallel to an edge when situated near the edge.

When a specimen was sectioned, coating cracks can sometimes be observed running parallel and near the substrate, but not through the interface. A crack of this type in a D1 coating (0.04" thick) is shown in Figures 18 and 19. In Figure 19, the coating-substrate bonding appears continuous in the vicinity of the crack.

Separations also took place at the coating-substrate interface itself. This can be seen at the end of the specimen in Figure 18. The inner surface of a portion of D2 coating (0.02" thick) pried away from the substrate can be seen in Figure 20. Note that this surface is quite similar in appearance to the outer coating surface and is unlike the coarser grained interior. A cross-section of a D2 specimen is shown in Figure 21.

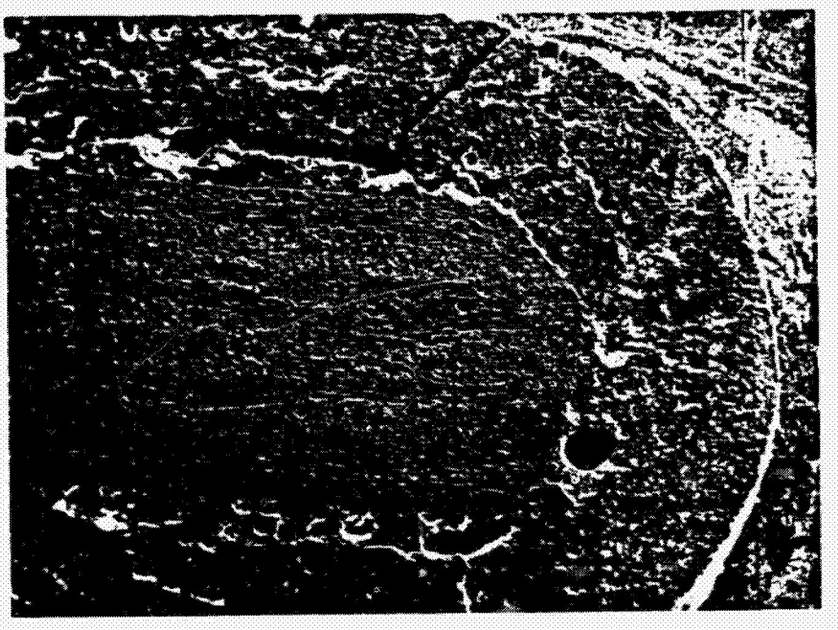

Figure 18. Type D1 specimen section, 20 X.

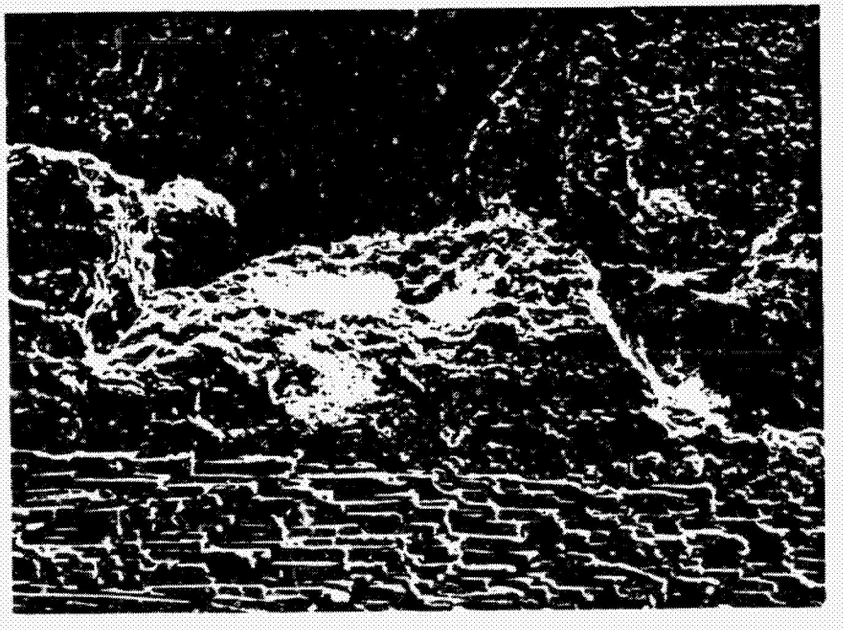

Figure 19. Type D1 coating-substrate interface, 200 X.

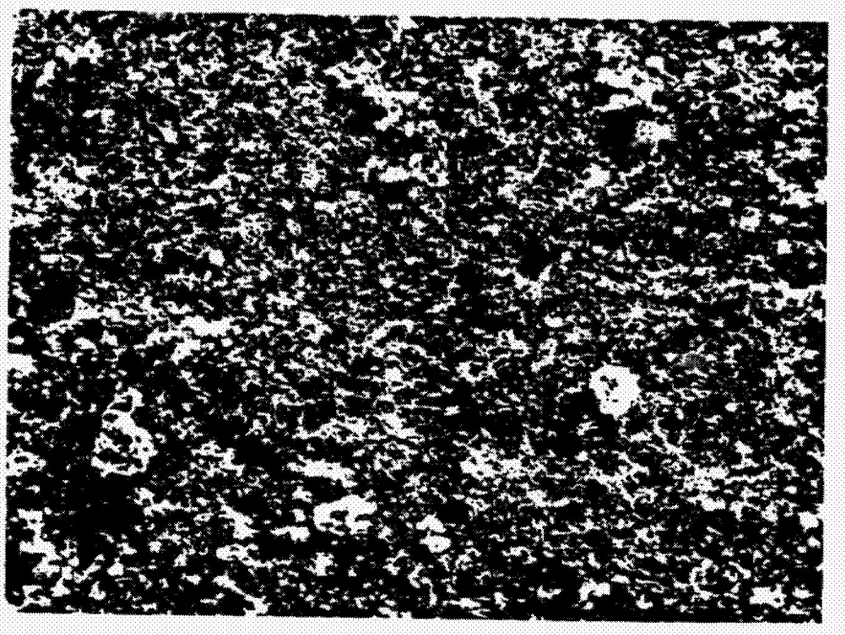

Figure 20. Type D2 coating inner surface, 200 X.

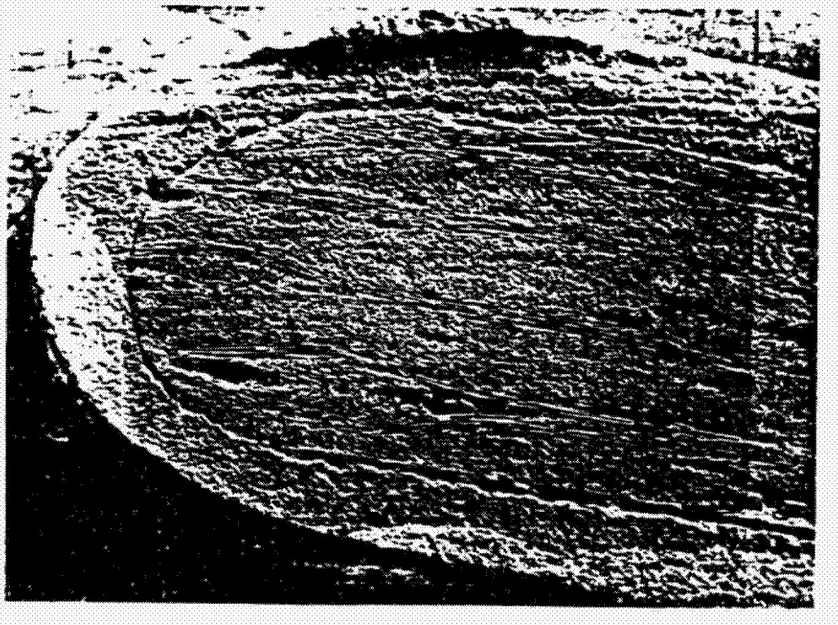

Figure 21. Type D2 specimen section, 20 X.

Figure 22. Type D3 coating inner surface, 200 X.

Oxidative roughening in D3 specimens was done to enhance coating adhesion to the substrate, even though work done on RCC indicated that the results could be variable. Figure 22 shows the inner surface of D3 type coating which has been pried away from the substrate. Note that the fracture surface has a rougher appearance than a corresponding surface from a D2 coating (240 grit substrate roughening only), as in Figure 20.

Coating types E1 through E4 (reduced nitridation temperatures) were omitted from further testing. Type E1 appeared identical to specimens which had been nitrided at 1350°C for 12 hours. As nitridation temperatures were reduced for types E2 through E4, the coatings went from light gray to grayish black and became increasingly susceptible to abrasion, indicating incomplete nitridation. However, even the E4 coating (minimum nitridation temperature) was cracked.

Coating types F1 through F3 (boron additions to green coating) were somewhat more successful. The F1 coatings, which used a Si green coating over a Si - 5.0 B primer, were similar in appearance to the D types. The F2 and F3 specimens, using Si - 2.5 B and Si - 5.0 B green coatings respectively, had a mottled appearance and were susceptible to abrasion. Nonethless, these were subjected to oxidation tests later.

2. Densified Coating

The triply densified G type coatings took on a black coloration around the specimen edges during post-impregnation heat treatment. Presumably the coloration is a result of the decomposition of the organosilicon densifier. Table 5 lists specimen mass prior to

TABLE 5

Initial Mass and Cumulative Gains

Over 3 Densifications

		Mass gain, g(%) after densification cycle		
Specimen	Initial Mass, g	1	2	3
G - 1	1.6400	0.0318 (1.94)	0.0371 (2.26)	0.0388 (2.37)
2	1.6500	0.0325 (1.97)	0.0386 (2.34)	0.0410 (2.48)
3	1.8453	0.0330 (1.79)	0.0402 (2.18)	0.0417 (2.26)

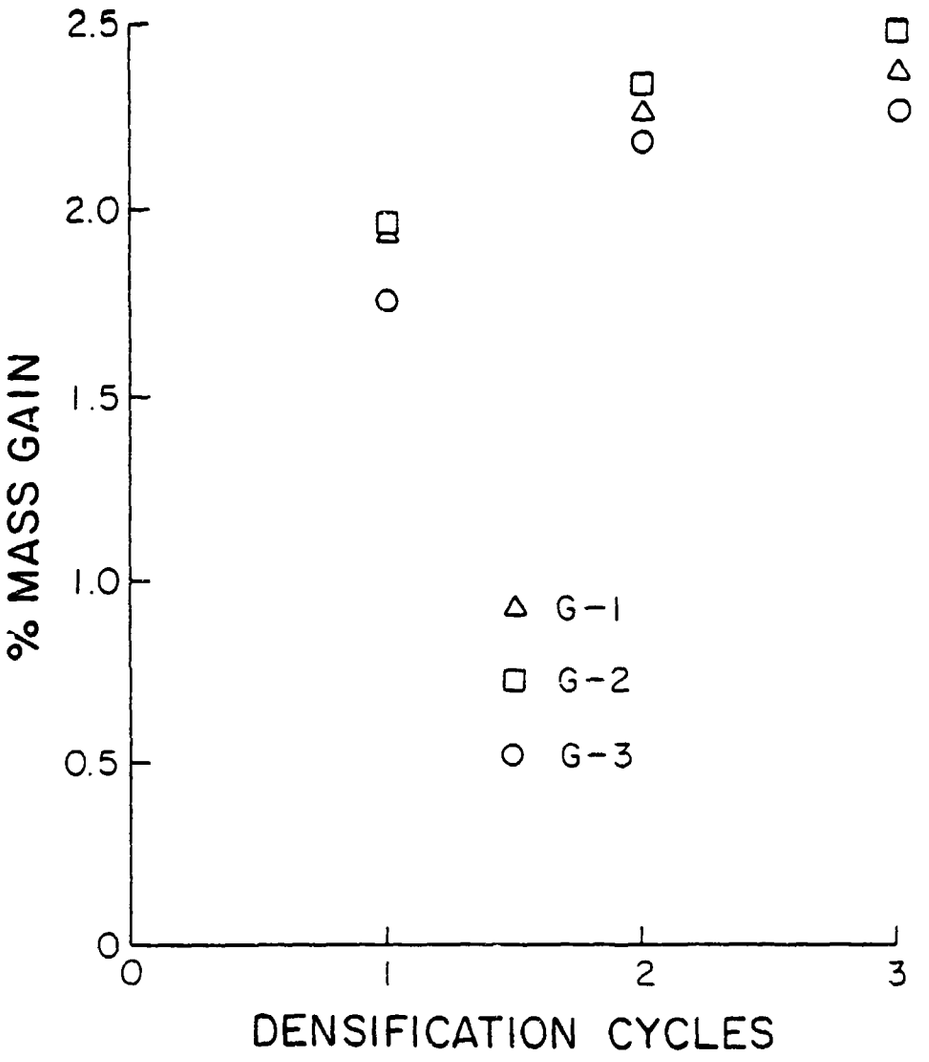

FIGURE 23. PERCENT MASS GAIN FOR TYPE G SPECIMENS DURING DENSIFICATION.

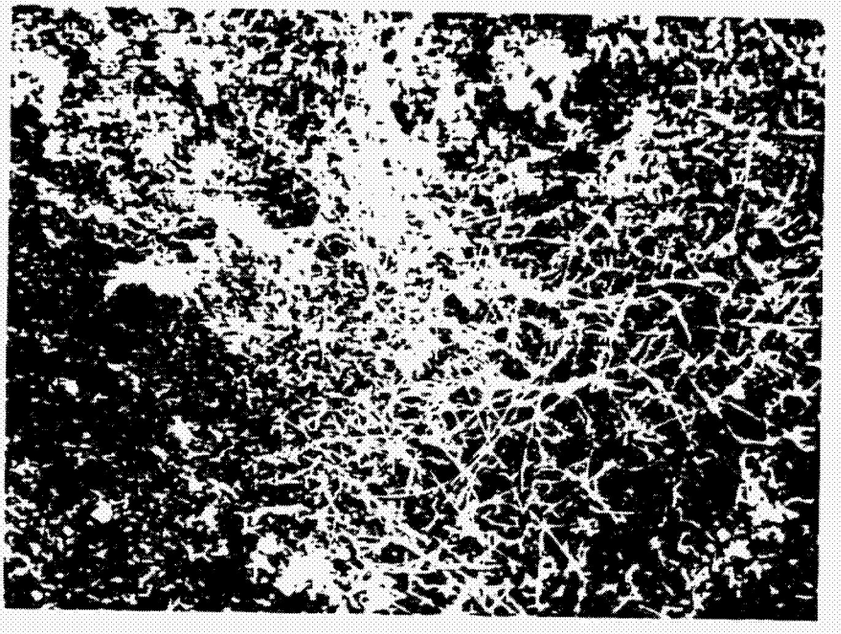

Figure 24. Type G coating surface, 1000 X.

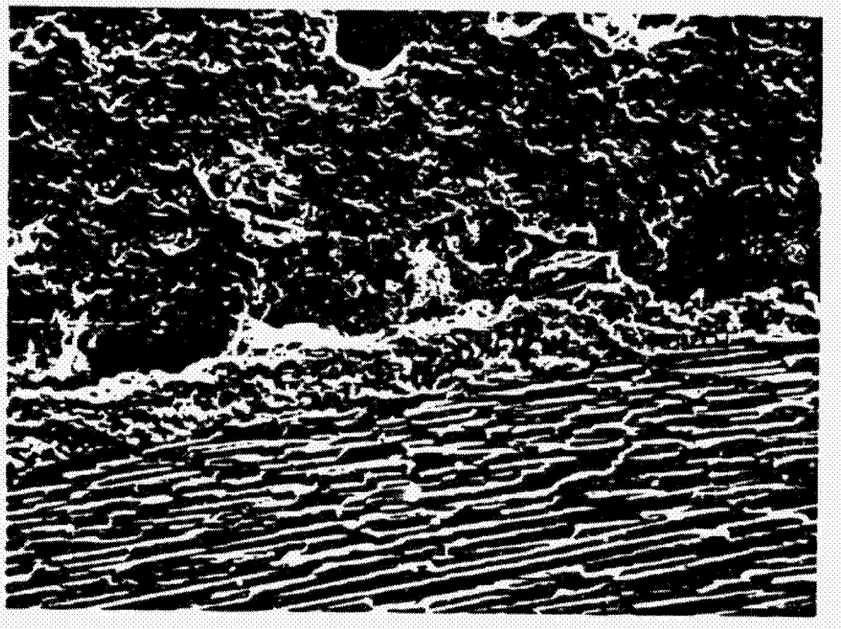

Figure 25. Type G coating-substrate interface, 200 X.

Figure 26. Type G coating-substrate interface, 1000 X.

densification and mass gains for each densification cycle. Percent densification mass gain for individual specimens is listed in Table 5 and plotted in Figure 23.

The surface of a triply densified specimen is shown in Figure 24. Note that the surface possesses some large grains as well as whiskers, and that the whiskers are more variable in size and density than those of predensified material, such as is seen in Figure 3. Shown in Figure 25 is a section through the coating-substrate interface of a G type specimen. Figure 26 is a higher magnication view of the same specimen and shows whiskers growing out into the coating-substrate separation.

3. Sealed Coatings

The H1 through H3 sealed coatings were not considered successful although the H2 coatings were subjected to oxidation tests. The desired result was a surface made impermeable by surface wetting and impregnation by liquid silicon. This did not occur in types H1 (1-5 micron Si sealant, 1 atm Ar) and H3 (-25 mesh Si sealant, low P Ar). In these specimens the silicon melted and coalesced without spreading over the surface. In type H2 (1-5 micron Si sealant, low P Ar), the silicon appeared to have vaporized completely along with the boron wetting agent. However, there was an average coating weight gain of 12.7%.

B. Results of ACC Oxidation Tests

Oxidation test cycles for ACC specimens were terminated when total percent mass loss reached approximately 25%, a figure well beyond the actual use level. As with the RCC specimens, the mass

loss/area is calculated using a nominal surface area for all specimens, and should be considered an approximation. The average percent mass loss for all ACC specimens is plotted in Figure 27. Individual specimen mass and mass losses are listed in Table 6, and the average six hour oxidation mass loss/area approximations are listed in Table 7.

1. Basic Coatings

One of the more protective ACC coatings came from the group of basic coatings; however, none of the ACC specimens were able to match the RCC. The basic ACC coating exhibiting the lowest mass loss was the D1 type, which comprised a 0.04" thick coating of 100% silicon on an abrasively roughed substrate. A section through the interface of an oxidized D1 specimen is shown in Figure 28; and features typically associated with oxidation damage are visible. These are the large vertical crack intersecting an area in which coating separation has taken place, and, below the primed layer, fibers left bare by matrix oxidation. The primed layer apparently possesses good oxidation resistance, and x-ray photoelectron spectroscopic analysis of primed substrate surfaces indicates the presence of silicon and lesser amounts of silicon carbide.

Of the D type specimens, the highest mass loss was exhibited by the D2 coatings. These were processed in the same manner as D1; however, thinner (0.02") coatings were applied.

The D3 coatings (0.02" silicon on an oxidatively roughened surface) offered apparent improvement in oxidation resistance over the D2 type. Coatings on oxidatively roughened substrates seemed to adhere best at the edges of the specimens, and an area of favorable

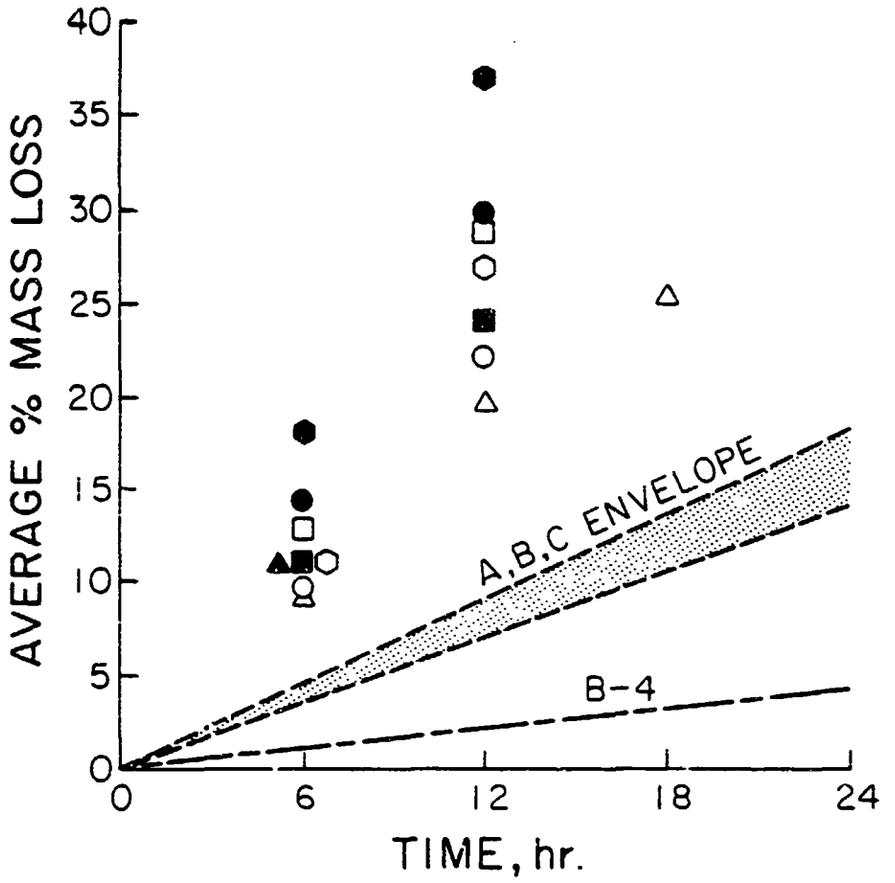

○ D1 0.04"
● D2 0.02" BASIC
● D3 0.02"/OXIDATION

□ F1 0 B
▲ F2 2.5B 0.04" BASIC/BORON ADDED
■ F3 5.0B

△ G 0.02" DENSIFIED

○ H2 0.02" SEALED

FIGURE 21. 1000 F MASS LOSS FOR TYPES D,F,G,H.

TABLE 6

Coated Mass and Mass Loss for Individual ACC Specimens

		Total Mass Loss, g(%), at Time, hr.		
Specimen	Coated Mass (g)	6	12	18
D1 - 1	1.0248	0.0925 (9.03)	0.2231 (21.77)	
2	1.1148	0.0927 (8.32)	0.2235 (20.14)	
3	1.0342	0.1007 (9.74)	0.2335 (22.58)	
4	0.9566	0.1034 (10.81)	0.2276 (23.70)	
avg.		(9.48)	(22.05)	
D2 - 1	1.9048	0.3308 (17.37)	0.8209 (43.10)	
2	1.7484	0.3284 (18.78)	0.5486 (31.38)	
avg.		(18.08)	(37.24)	
D3 - 1	1.8093	0.3330 (18.40)	0.5774 (31.91)	
2	1.7893	0.2275 (12.71)	0.5057 (28.26)	
3	1.7867	0.2256 (12.63)	0.4540 (25.41)	
4	1.8115	0.2443 (13.49)	0.6075 (33.97)	
avg.		(14.31)	(29.89)	
F1 - 1	1.9355	.2234 (11.54)	.4541 (23.46)	
2	1.8013	.2185 (12.13)	.5352 (29.71)	
3	1.8350	.2738 (14.92)	.6138 (33.45)	
avg.		(12.86)	(28.87)	
F2 - 1	1.9945	.2192 (11.19)		
2	2.2625	.2373 (11.79)		
3	2.2313	.2077 (9.54)		
avg.		(10.84)		
F3 - 1	1.9574	.2297 (11.52)	.4752 (23.83)	
2	2.0122	.1998 (8.83)	.4556 (20.14)	
3	2.1767	.2913 (13.06)	.6113 (27.40)	
avg.		(11.14)	(23.79)	

TABLE 6. continued

Specimen	Coated Mass (g)	6		12		18	
G - 1	1.6788	.1478	(8.80)	.3231	(19.25)	.4183	(24.92)
2	1.6910	.1585	(9.37)	.3327	(19.67)	.4303	(25.45)
avg.			(9.08)		(19.46)		(25.18)
H2 - 1	2.1635	.2158	(9.97)	.5166	(23.88)		
2	2.0664	.2523	(12.21)	.6426	(31.10)		
avg.			(11.09)		(27.49)		

TABLE 7

Calculated ACC Mass Loss/Area for 6 hr. Oxidation

at 1000°F in Air

Specimen	Nom. Area, in^2	6 hr. Avg. Loss, g	6 hr. Mass Loss, lb/ft^2
D1 - 1234 Avg.	.84	.0973	.036
D2 - 12 Avg.	1.45	.3296	.072
D3 - 1234 Avg.	1.45	.2576	.056
F1 - 123 Avg.	1.45	.2386	.052
F2 - 123 Avg.	1.45	.2214	.048
F3 - 123 Avg.	1.45	.2403	.053
G - 12 Avg.	1.45	.1531	.033
H2 - 12 Avg.	1.45	.2341	.051

Figure 28. Type D1 coating-substrate interface, oxidized 12 hours at 1000°F, 200 X.

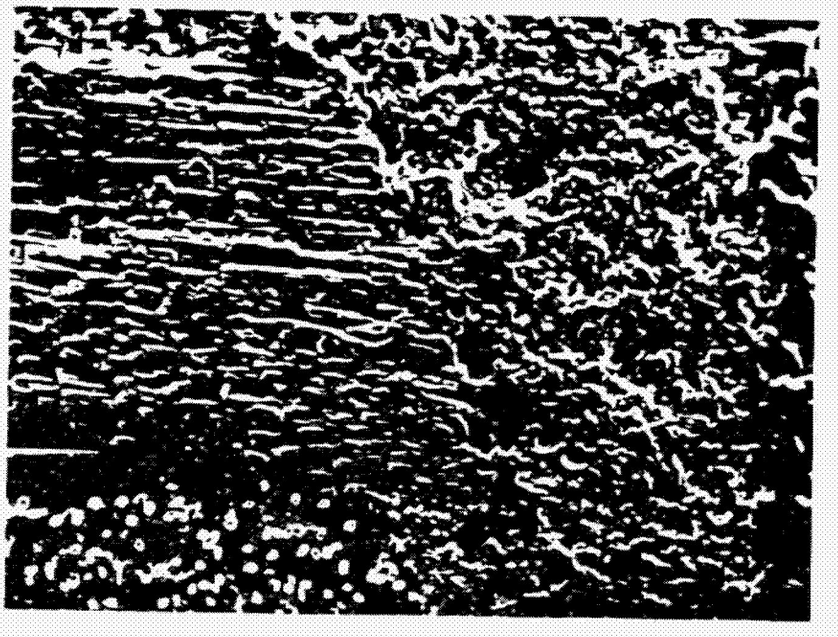

Figure 29. Type D3 coating-substrate interface, oxidized 12 hours at 1000°F, 200 X.

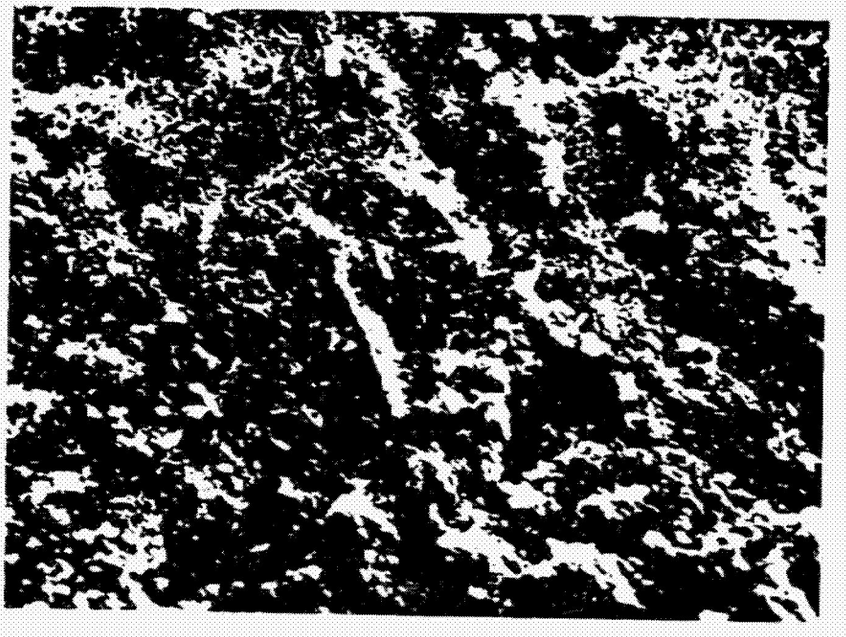

Figure 30. Type G coating surface, oxidized 18 hours at 1000°F, 1000 X.

bonding in a D3 specimen (exposed to oxidation) is shown in Figure 29.

Coating types F1 through F3 (boron-containing primer and/or green coating) did not seem to offer the oxidation protection of the D1 type. The F type coatings are basically D1 types with boron additions, and, although the coating thickness were approximately equal, mass loss rates for F type coatings were generally higher. All of the F types performed approximately the same, regardless of boron content.

2. Densified Coatings

The mass loss rates for the triply densified G type coatings were lower than those of the D2 coatings, and were approximately equal to those of the D1 specimens. The G coating is a densified 0.02" thick D2 coating; the D1 coating is processed like the D2 but is 0.04" thick. The surface of an oxidized G type coating is shown in Figure 30.

3. Sealed Coatings

The "sealed" H2 coatings were another modification of the D2 coatings, and they performed slightly better than D2. H2 mass loss rates were similar to those of the F type, which received boron additions prior to nitridation, rather than after nitridation as the H2 coatings had.

VIII. Discussion

In terms of percentage mass loss and mass loss/area, the A, B, and C type coatings applied to RCC offered much better performance in oxidizing conditions than did the D, F, G, and H type coatings applied to ACC. The Vought mass loss standard (0.013 lb/ft^2 lost over 6 hours of oxidation at $1000^{\circ}F$ in air) was the result of tests on ACC which had been SiC coated, TEOS impregnated, and sealed with a proprietary overcoat. The RCC substrate specimens (types A, B, C) had been previously impregnated with TEOS, whereas the ACC substrate specimens (types D, E, F, G, H) had not.

Since TEOS impregnation was developed to increase the oxidation resistance of the substrates, the ACC specimen would have probably performed better had they been previously impregnated. In addition, the ACC specimens possessed a lower coefficient of thermal expansion than RCC. This leads to an assumption of higher coating stresses than in the higher expansion RCC specimens. While none of the RCC specimens exhibited obvious cracks on the coating surface, all of the ACC specimens did. Overall, the Si_3N_4 coated RCC specimens approximately equalled the $1000^{\circ}F$ performance of ACC coated by Vought, whereas the Si_3N_4 coated ACC specimens fell far short of this mark.

The cracking of the coatings on ACC may also occur prior to nitridation. This is supported by the cracking of the E4 type coating (nitrided at $1150^{\circ}C$ for 36 hr.), which was cracked though little or no nitridation took place, and by a comparison of Figure 3 with Figures 17 and 19. Figure 3 shows the typical fibrous appearance which results when nitridation takes place at a free surface, whereas

nitrided silicon below the surface possesses a denser, granular appearance. The surfaces shown in Figures 17 and 19 were adjacent to the substrate, yet they closely resemble the free surface shown in Figure 3. This suggests that some separation between the green coating and the ACC substrate could have taken place prior to nitridation.

Such a separation could be caused by thermal expansion differences between the green coating and the ACC substrate. The coefficient of thermal expansion of silicon is approximately 4.1 x $10^{-6}/^{o}C$ from 200^{o} to $1400^{o}C$ (2). During furnace heat-up, the green silicon coating would expand at a higher rate than the substrate, creating compressive stresses in the green coating parallel to the substrate surface. This compression could result in an outward buckling and separation between coating and substrate. A coating affected in this manner would probably afford less protection than one simply cracked through to an intact interface. Some support is lent to this view by the fact that the mass loss rates for D2 specimens (0.02" coating on abrasively roughened substrate) appear to be higher than those for D3 specimens (0.02" coating on oxidatively roughened substrate). Oxidative roughening results in the exposure of fiber ends which seem to be able to anchor the coating to some extent, and the D3 coating did offer improved protection over the D2 type. Coating adhesion could perhaps be improved by nitriding specimens under light constraint, such as in an inert powder pack, rather than in a free standing condition.

Silazane densification of RSSN coatings showed potential on a microstructural basis (Figures 5, 6) and on a performance basis (specimen B-4); however, process uniformity was apparently not achieved. There did not appear to be an appreciable crack-filling effect when coatings on ACC were densified. However, oxidation protection seemed better in the type G specimens relative to similar but non-densified D2 specimens, indicating that mass loss rates were sensitive to coating density even in the presence of large cracks.

Inomata (9) has demonstrated that the oxidation resistance of RSSN can be markedly increased by surface impregnation with molten silicon under one atmosphere of nitrogen. The failure to provide a fully satisfactory silicon scaled RSSN coating may be due to impurities in the silicon and/or to traces of oxygen in the process gases. The 1-5 micron silicon powder was analyzed by x-ray diffraction and appeared to contain minor contaminants which could not be identified.

IX. Conclusions

1. Using lower temperatures than in the present SiC coating process, crack free reaction sintered silicon nitride coatings can be applied to Vought Corporation's RCC composite.
2. In 1000°F air oxidation conditions, TEOS impregnated RCC with a 0.04 inch RSSN coating yields approximately the same mass loss rate as industry standard ACC which has been SiC coated, TEOS impregnated, and overcoated.
3. The thermal expansion coefficient of ACC is too low relative to Si or RSSN to form crack free RSSN coatings on ACC by the methods employed; the resulting mass loss rate is unacceptably high for ACC which has not been TEOS impregnated.
4. Silazane densification and silicon sealing can increase the oxidation protection offered by RSSN coatings on RCC and ACC; however, the methods employed did not allow for optimum process conditions.
5. Areas of further study include methods of preventing coating-substrate separation during processing, densification and sealing process optimization, and reactive formation of SiC coatings at much lower temperatures than those presently employed.

X. Literature Cited

1. J. Mukerji and B. S. Biswas, "Effect of Iron, Titanium, and Hafnium on Second-Stage Nitriding of Silicon". Journal of the American Ceramic Society; N. 64, No. 9, 1980, . 549.

2. J. F. Lynch, C. G. Ruderer, and W. H. Duckworth, eds., Engineering Properties of Selected Ceramic Materials. Columbus, Ohio: The American Ceramic Society, Inc., 1966.

3. I. E. Campbell and E. M. Sherwood, eds., High Temperature Materials and Technology. New York, New York: John Wiley and Sons, Inc., 1967.

4. F. L. Riley, ed., Nitrogen Ceramics. Reading, Massachusetts: Noordhoff International Publishing, 1977.

5. C. M. B. Henderson and D. Taylor, "Thermal Expansion of the Nitride and Oxynitride of Silicon in Relation to their Structures", Transactions of the British Ceramic Society, V. 74, No. 2, 1975, p. 49.

6. M. Mitomo and J. H. Sharp, "Oxidation of α and β Silicon Nitride", Yogyo Kyokai Shi, V. 84, No. 1, 1976, p. 41.

7. A. G. Evans and R. W. Davidge, "The Strength and Oxidation Resistance of Reaction Sintered Silicon Nitride", Journal of Materials Science, V. 5, 1970, p. 314.

8. T. Hirai, K. Niihara, and T. Goto, "Oxidation of CVD Si_3N_4 at 1550° to 1650°C", Journal of the American Ceramic Society, V. 63, No. 7-8, 1980, p. 419.

9. Y. Inomata, "Oxidation Resistance of Si-Impregnated Surface Layer of Reaction Sintered Silicon Nitride Articles", Yogyo Kyokai Shi, V. 1, No. 83, 1975, p. 9.

10. H. D. Batha and E. D. Whitney, "Kinetics and Mechanism of the Thermal Decomposition of Si_3N_4", Journal of the American Ceramic Society, V. 56, No. 7, 1972, p. 365.

11. T. J. Whalen and A. T. Anderson, "Wetting of SiC, Si_3N_4, and Carbon by Si and Binary Si Alloys", Journal of the American Ceramic Society, V. 58, No. 9-10, 1975, p. 396.

12. J. C. Swartz, "Atmospheric Effects on Wetting of Si_3N_4 by Liquid Si", Journal of the American Ceramic Society, V. 59, No. 5-6, 1976, p. 272.

13. K. S. Mazdiyasni, R. West, and L. D. David, "Characterization of Organosilicon-Infiltrated Porous Reaction Sintered Silicon Nitride", Journal of the American Ceramic Society, V. 61, No. 11-12, 1978, p. 504.

14. F. S. Galasso, "Pyrolytic Silicon Nitride Prepared from Reactant Gases", Powder Metallurgy International, V. 11, No. 1, 1979, p. 7.

15. J. J. Gebhardt, R. A. Tanzilli, and T. A. Harris, "Chemical Vapor Deposition of Silicon Nitride", Journal of the Electrochemical Society, V. 23, No. 10, 1976, p. 1578.

16. M. E. Washburn, "Silicon Oxynitride Refractories", American Ceramic Society Bulletin, V. 46, No. 7, 1967, p. 667.

17. T. C. Ehlert, T. P. Dean, M. Billy, and J. C. Labbe, "Thermal Decomposition of the Oxynitride of Silicon", Journal of the American Ceramic Society, V. 63, No. 3-4, 1980, p. 235.

18. M. J. Rand and J. F. Roberts, "Silicon Oxynitride Films from the $NO-NH_3-SiH_4$ Reaction", Journal of the Electrochemical Society, V. 120, No. 3, 1973, p. 446.

19. M. H. Lewis and P. Barnard, "Oxidation Mechanisms in Si-Al-O-N Ceramics", Journal of Materials Science, V. 15, 1980, p. 443.

20. M. Mitomo, Y Yajima, and N. Kuramoto, "Thermal Decomposition of Si-Al-O-N Ceramics", Journal of the American Ceramic Society, V. 62, No. 5-6, 1979, p. 316.

Vita

The candidate, Yoshio Robert Yamaki, was born on January 22, 1955 in Wahiawa, Hawaii. He received a degree of Bachelor of Science in Ceramic Engineering from Virginia Polytechnic Institute and State University in June, 1977. This was followed by employment at Kentron International in Hampton, Virginia. The candidate will be returning to Kentron after the completion of degree requirements.

Yoshio Robert Yamaki